Removal of copper from aqueous solutions by biosorption onto pine sawdust

Clara Isabel Orozco, M. Sonia Freire, Diego Gómez-Díaz, Julia González-Álvarez [*]

Department of Chemical Engineering, School of Engineering, Universidade de Santiago de Compostela, Santiago de Compostela, 15782, Spain

ARTICLE INFO

ABSTRACT

Untreated *Pinus radiata* sawdust was investigated for the removal of Cu^{+2} ions from aqueous solutions. The biomass was characterized by Inductively Coupled Plasma-Mass (ICP-MS) spectrometry and by Scanning Electron Microscopy with an Energy Dispersive X-ray spectroscopy (SEM-EDX), X-Ray crystalline powder Diffraction (XRD) and Fourier Transform Infrared (FTIR) spectroscopy, before and after adsorption. The influence of contact time (up to equilibrium), adsorbent dose (1–50 g/L), initial metal ion concentration (5–300 mg/L) and pH (2–8) on copper sorption efficiency was studied through batch experiments. The results demonstrated that adsorption equilibrium is reached in less than 2 h and the best conditions (Cu^{+2} removal percentage, 93.4% and adsorption capacity, 0.82 mg/g) were achieved by increasing the adsorbent dose up to 5 g/L and the solution pH up to 7, and decreasing the initial metal concentration to 5 mg/L. The adsorption was optimized by means of a Doehlert experimental design analyzing the influence of adsorbent dose (5–15 g/L) and copper initial concentration (5–45 mg/L) on adsorption efficiency. Kinetic data were satisfactorily fitted to the second-order kinetic model. Intraparticle diffusion model demonstrated that different stages are involved in the adsorption process. Langmuir isotherms fitted satisfactorily the copper bioadsorption equilibrium data. Desorption studies achieved high efficiencies up to 94.5% and the possibility of sawdust regeneration was studied with four adsorption-desorption cycles. Thus, this study evidenced that sawdust is a promising efficient, renewable and economic adsorbent for metal removal and its use for that purpose constitutes an alternative for its management and valorization.

1. Introduction

In the past decades, the fast growth of the industrial activity has promoted the discharge of pollutants in the surface and groundwater. Heavy metals can be distinguished from other pollutants for their serious implications on the environment and human health. A problem that is aggravated if it is considered that heavy metals are present in the discharge of numerous industries such as metal processing, mining, energy sector, surface treatment of metals and plastics, organic chemical industry, etc. (European Environment Agency, 2016).

This kind of pollutants is not only a serious environmental issue due to their high toxicity in trace concentrations but also due to their non-biodegradability, accumulation in the food chain, and mutagenic and carcinogenic effects (World Health Organization, 2006). For example, in the case of copper which is the metal with the largest toxicity factor in European waters (European Environment Agency, 2019), exposure to large doses in humans provokes degeneration or even necrosis of the kidneys, the liver, and

the gastrointestinal system. Moreover, it is related to nervous system alterations or mental problems like insomnia or anxiety (Briffa et al., 2020). Therefore, the current study will be focused on copper elimination due to its high emissions in industrial discharges (European Environment Agency, 2019). The ion selection is reinforced by copper properties, such as the ionic radius or electronegativity, which make it an ion within the group of heavy metals with average removal trends in current technologies, and a reference for the removal of other metals, although a specific study is recommended for each heavy metal (Gorgievski et al., 2013).

In response to these adverse effects, governments have implemented diverse regulations and standards to limit heavy metal discharges. In the European Union, remarkably, the last decision about these limits corresponds to the organizations of each member country, and the discharge limits depend mainly on the medium of discharge: the sewage system or a direct discharge to a river or sea. For example, in the case of Spain, the limits for copper discharge are between 0.25 and 3 mg/L for direct discharges and between 1 and 5 mg/L for sewerage (MARM et al., 2009). Although, the European trend for copper discharges is generally more restrictive, for example, in Poland or Belgium the limits discharges are under 1 mg/L (BiPRO, 2012; Poland Ministry of Agriculture, 2013). In other countries, the emission value trend is similar to Spain, like in the US where the direct discharges limits are between 1 and 5 mg/L, meanwhile, the indirect emissions are lower than 1 mg/L (U.S. EPA; ZDHC, 2015). However, all these limits can be altered in certain cases such as the presence of sensitive aquatic species, nearby drinking water intakes or specific industrial regulations (MARM et al., 2009). In addition, it is necessary to consider the presence of different pollutants in industrial wastewater: biodegradable organic matter, suspended solids, salts and other metals ions that could interfere with copper ions elimination (European Environment Agency, 2019; Lim et al., 2008). Anyway, the composition of industrial effluents presents a great variety taking into account the diversity of industries, processes or raw materials, being a variable difficult to investigate and requiring specific studies applied to each particular industry (Baskar et al., 2022).

Actual technologies for removing metals from wastewaters such as precipitation, ion exchange, membrane separation, etc. do not allow to achieve the discharge limits imposed due to several difficulties and limitations. These include high costs, sludge production, high reagent usage or energy requirements and low efficiency for heavy metals concentrations below 100 mg/L (Delgado Sancho et al., 2016). This is why efforts have been focused on developing more economical and effective methods, such as adsorption which arises nowadays as an opportunity for the removal of heavy metals and other pollutants for having numerous advantages, such as its low energy requirements or its operation simplicity (Abdolali et al., 2014).

Activated carbons are the most widely used adsorbents for removing water pollutants, but their high production cost and difficult regeneration have caused the search for cheaper and more eco-friendly options (Sahmoune and Yeddou, 2016). Compared to other adsorbents, waste biomass meets those requirements and its use as adsorbent provides an alternative for its valorization achieving a more environmentally friendly process and contributing to the circular economy. Thus, various studies have reported good results using various biomass for effluent metal removal: oyster shell waste powder (Wu et al., 2014), olive stone and pine bark (Blázquez et al., 2011), orange peels (Pérez-Marín et al., 2007), rice husk (Bansal et al., 2009), *Pinus sylvestris* sawdust (Taty-Costodes et al., 2003), etc.

Among a wide range of low-cost adsorbents, sawdust can be considered a promising alternative for being abundant, renewable and rich in different functional groups such as carbonyl, carboxylic, amine, and hydroxyl, which have shown favorable interactions between the metals ions and adsorbent surface (Meez et al., 2021). Sawdust also shows various potential characteristics of a good adsorbent, compared with agricultural wastes, such as high surface areas (Carreño-De León et al., 2017) or high cellulose and lignin contents, which are related to adsorption capacity (Abdolali et al., 2014; Basso et al., 2010). *Pinus radiata* is one of the coniferous species most widely spread across northern Spain and is common in other countries, such as USA, New Zealand or Chile, so large quantities of wastes are generated from its industrial processing (Castro et al., 1999; CIF Lourizan, 2017). Despite the high amount of *Pinus radiata* sawdust produced, studies focused on its use for the removal of pollutants from wastewater are limited, especially those in which the sawdust has not been pre-treated. Since lignocellulosic materials without previous modification have presented good removal efficiencies for metals removal (Acemioğlu and Alma, 2004; Mannaï et al., 2021; Semerjian, 2018), this research proposes the use of pine sawdust as a cheap and safe adsorbent, while reducing the utilization of hazardous reagents.

For that reason, this work aims to investigate the feasibility of using *Pinus radiata* sawdust (PS) without any pre-treatment for the removal of Cu^{+2} from aqueous solutions. To attain this objective, firstly, the adsorbent was characterized by different techniques (ICP-MS, SEM-EDX, FTIR and XRD). In a second stage, the influence of adsorbent dose (1–50 g/L), initial Cu^{+2} concentration (5–300 mg/L), pH (2–8), and contact time (till 24 h) on adsorption efficiency and capacity was analyzed using the one factor at a time method, and the effect of the most significant variables was studied using response surface methodology (RSM). In addition, adsorption kinetics and equilibrium were studied to understand the process. Finally, the efficiency of metal desorption and adsorbent reuse was analyzed.

2. Material and methods

2.1. Adsorbent and adsorbate

2.1.1. Adsorbent preparation and characterization

PS was provided by a regional sawmill (Lugo, Spain). It was sun-dried for 24 h (moisture content 10% dry basis), subsequently sieved and the fraction between 0.5 and 1 mm was selected. PS was used in the different studies without any further treatment.

In previous studies, the point of zero charge (pH_{PZC} = 4.8) was determined as described by Nordine et al. (2014) and Şentürk and Alzein (2020). Also, sawdust BET surface areas from N_2 adsorption isotherm at 77 K (1.55 ± 0.81 m²/g) and CO_2 adsorption isotherm at 273 K (17.83 ± 0.032 m²/g) were determined (sent to publication). Heavy metals in sawdust that could interfere with the adsorption process were quantified by Inductively Coupled Plasma (ICP) with a plasma mass spectrometer (ICP-MS Agilent 7900).

Additionally, the surface morphology and elemental composition of the sawdust before and after copper adsorption were analyzed by Scanning Electron Microscopy and Energy Dispersive X-ray spectroscopy (SEM-EDX) (ZEIS EVO LS 15 with EDX).

In addition, Fourier transform infrared (FTIR) spectra for pine sawdust, before and after adsorption, were recorded with a VARIAN FTIR 670 spectrometer to examine those functional groups responsible for copper adsorption. KBr pellets (1%, g of sample per 100 g of pellet) were prepared with samples after grinding and drying under vacuum for five days. Cu-loaded sawdust sample analyzed was obtained at an adsorbent dose of 12.5 g/L, pH = 7 and an initial copper concentration of 45 mg/L for 2 h at 25 °C.

X-ray crystalline powder diffraction (XRD) data were collected at room temperature, in Bragg-Brentano geometry using a BRUKER D8 ADVANCE type X-ray diffractometer (40 kV, 40 mA, theta/theta) equipped with a sealed X-ray tube (CuKα1, λ = 1.5406 Å), and a LYNXEYE XE-T type detector. The diffractograms were obtained in the angular range of $5 < 2\Theta < 50°$ with a step of 0.02° at 2 s per step. The samples were rotated during the measurement to obtain the most optimal peak profiles for the analysis, as well as to minimize the effect of the preferred orientation (Yao et al., 2020). They were deposited on a base of an oriented crystal (Si 511 plate) to avoid the background noise caused by a glass-like support. The crystallinity index (CI) was determined as Bala and Mondal (2018).

2.1.2. Preparation of metal solutions

Cu^{+2} solutions for adsorption experiments were prepared by dissolving $Cu(NO_3)_2 \cdot 3H_2O$ in distilled water at the corresponding concentration. Copper solutions for calibration were prepared from a copper stock solution (1 mg/mL) in 1% nitric acid. When necessary, the solution pH was modified using 0.01 M and 1 M HNO_3 or 0.1 M and 1 M NaOH solutions.

2.2. Batch adsorption experiments

Batch adsorption experiments were performed by placing 50 mL of the copper solution and the appropriate amount of adsorbent according to the dose selected in an orbital shaking bath (J.P Selecta Unitronic Vaivén C) at 25 °C and 100 rpm. After reaching the target contact time, the samples were vacuum filtered using glass microfiber filters (1.2 μm) and the residual copper concentration was determined by Flame Atomic Absorption Spectrophotometry (GBC 932 A A). All experiments were duplicated, and copper concentration was measured in triplicate to ensure the repeatability of the results.

Adsorption efficiency (%) and capacity (qt, mg/g) were calculated using the equations Eq. (1) and Eq. (2), respectively:

$$\text{Adsorption efficiency } (\%) = \left(\left(C_0 - C_t \right) / C_0 \right) x100 \tag{1}$$

$$q_t \, (mg/g) = \left(\left(C_0 - C_t \right) / m \right) xV \tag{2}$$

where C_0 and C_t are the initial and residual metal concentration after a predetermined time (mg/L), respectively, m (g) is the mass of dry adsorbent and V (L) is the volume of the metal aqueous solution.

2.2.1. Influence of different variables on copper adsorption

In this investigation, the influence of several variables on adsorption efficiency was studied, namely, contact time, adsorbent dose, initial Cu^{+2} concentration, and pH (Afroze and Sen, 2018; Meez et al., 2021).

Firstly, the effect of contact time (up to 24 h) on copper adsorption was studied, fixing the other variables: natural pH (5.4); adsorbent dose (1 or 50 g/L) and initial copper concentration (5, 45 and 300 mg/L). In a second stage, the effect of the adsorbent dose (1, 5, 10, 25 and 50 g/L) was studied for a 5 mg/L copper initial concentration at natural pH and a contact time of 2 h. Then, the effect of the initial metal concentration was studied for a copper concentration of 1 and 5 mg/L with an adsorbent dose of 5 g/L at natural pH and a contact time of 2 h. Finally, the effect of pH (2, 4, natural (5.4), 6, 7, 8) was investigated for an initial copper concentration of 5 mg/L, an adsorbent dose of 5 g/L and a contact time of 2 h. All the experiments were performed following the procedure previously described.

2.2.2. Experimental design

A Doehlert experimental design was applied, following the Response Surface Methodology (RSM), to appraise the combined effects of the factors that most influence adsorption efficiency. The variables selected for the optimization were the adsorbent dose (X_1), which was studied at five levels (5, 7.5, 10, 12.5, and 15 g/L) and the initial metal concentration (X_2), evaluated at three levels (5, 25, and 45 mg/L). The other parameters to consider in this investigation, pH (natural or 7) and time (2 h, time till equilibrium determined in Section 3.2.1), were fixed. The values selected for the independent variables and their coded values are presented in Table 1. The mathematical-statistical analysis was performed with the IBM SPSS Statistics software (Version 25 for Windows). The experimental data can be described, with the next quadratic equation (Eq. (3)) for two variables (Bezerra et al., 2008).

Table 1
Doehlert experimental design parameters for copper adsorption efficiency.

Factor	Variable	Unit	Coded level				
			−1	−0.5	0	0.5	1
				−0.866	0	0.866	
X_1	Adsorbent dose	g/L	5	7.5	10	12.5	15
X_2	Initial copper concentration	mg/L		5	25	45	

$$Y = \beta_0 + \beta_1 X_1 + \beta_2 X_2 + \beta_{12} X_1 X_2 + \beta_{11} X_1^2 + \beta_{22} X_2^2 \tag{3}$$

where Y is the response (copper adsorption efficiency); β_0, the constant term; β_1 and β_2, the regression coefficients for the linear effects; β_{12}, for the interaction effect; β_{11} and β_{22}, for the quadratic effects and X_1 and X_2 represent the independent variables (the adsorbent dose and the initial copper concentration, respectively).

In order to determine the significant factors, an analysis of variance (ANOVA) was carried out establishing a 95% confidence level ($p < 0.05$). Meanwhile, the model significance was evaluated with the coefficient of determination (R^2) and the adjusted R^2_{adj}.

2.3. Adsorption kinetics

The adsorption kinetic studies allow to determine the mechanism of the adsorption process. Various adsorption kinetic models have been proposed, being the most employed for identifying the adsorption dynamics the pseudo-first-order (PFO) model or Lagergren model, the pseudo-second-order (PSO) or Ho's model and the intra-particle (IP) model (Lima et al., 2015; Kajjumba et al., 2018).

The pseudo-first-order kinetic model, which is often related to physical sorption, can be described by the differential and linearized equations (4) and (5):

$$dq_t/dt = k_1 \left(q_e - q_t \right) \tag{4}$$

$$\ln \left(q_e - q_t \right) = \ln q_e - k_1 t \tag{5}$$

The pseudo-second-order kinetic model, which considers the chemical sorption as the rate-limiting step, uses the differential and linearized equations (6) and (7):

$$dq_t/dt = k_2 \left(q_e - q_t \right)^2 \tag{6}$$

$$t/q_t = 1/k_2 q_e^2 + t/q_e \tag{7}$$

where q_e and q_t are the amount adsorbed at equilibrium and at time t (mg/g), respectively; k_1, the PFO constant (min^{-1}); k_2, the PSO constant (g/mg min); and t, time (min).

Nevertheless, these models don't provide information for the diffusion mechanisms and since adsorption is controlled by the slowest step, it is interesting to know which is the rate-limiting step. Intraparticle diffusion, compared with the other steps, possibly offers higher resistance to mass transfer so it is important to confirm this assumption applying the IP model expressed by Eq. (8) (Lima et al., 2015; Sahoo and Prelot, 2020):

$$q_t = k_c t^{0.5} + C \tag{8}$$

where k_c is the intraparticle diffusion constant (mg/g min$^{0.5}$) and C is a constant that determines the thickness of the boundary layer (mg/g). If the plot corresponding to the equation passes through the origin, intraparticle diffusion is the rate-limiting step. However, when the plot shows multiple linear sections it implies that the adsorption process is controlled by different mechanisms (Lima et al., 2015; Kajjumba et al., 2018).

To modelize copper adsorption kinetic data from experiments described in Section 2.2.1 were used.

2.4. Adsorption equilibrium

Adsorption isotherms provide a wide variety of information such as the affinity and interactions between the adsorbent and adsorbate or the value of the adsorbent capacity. In the present study, the copper adsorption on the PS surface was analyzed with Langmuir and Freundlich isotherm models.

Langmuir model assumes that adsorption is monolayer and the adsorbents have a finite number of active sites, which are homogeneously arranged on the surface and are energetically equivalent. The Langmuir isotherm equation is described by Eq. (9) and its linearized expression in Eq. (10) (Lima et al., 2015):

$$q_e = \left(q_m K_L C_e \right) / \left(1 + K_L C_e \right) \tag{9}$$

$$C_e/q_e = \left(1/K_L q_m \right) + C_e/q_m \tag{10}$$

where q_e and q_m are the equilibrium and maximum adsorption capacity (mg/g), respectively; K_L, the Langmuir adsorption constant (L/mg) and C_e, the adsorbate concentration in the equilibrium (mg/L).

Furthermore, the dimensionless separation or equilibrium parameter, R_L, which can be calculated using Eq. (11), can be used to know more characteristics about adsorption. According to literature (Afroze and Sen, 2018) adsorption can be: irreversible ($R_L = 0$), favorable ($0 < R_L < 1$), linear ($R_L = 1$) or unfavorable ($R_L > 1$).

$$R_L = 1 / \left(1 + K_L C_0 \right) \tag{11}$$

Freundlich model is characteristic of adsorbents that have active sites with different affinities or adsorption energies. Furthermore, it is assumed that the adsorption can be multilayer. This model can be expressed with Eq. (12) or with its linearized version in Eq. (13):

$$q_e = K_F C_e^{\frac{1}{n}} \tag{12}$$

$$\ln q_e = \ln K_F + 1/n \ln C_e \tag{13}$$

where K_F is Freundlich adsorption constant which is an indicator of adsorption capacity (mg/g (mg/L)$^{-1/n}$); and n, describes the affinity between adsorbent and adsorbate. If the value of n is lower than 1, adsorption is unfavorable; by contrast, when n > 1, the adsorption of the molecules onto the adsorbent surface is favorable. High values of n suggest a strong sorption intensity.

Equilibrium studies were performed at 25 °C and natural pH with an adsorbent dose of 5 g/L, varying the initial copper concentration between 5 and 360 mg/L and with a contact time of 2 h following the procedure previously described.

2.5. Adsorbent regeneration

Regeneration experiments were performed using adsorption conditions selected from the previous experiments (solid/liquid ratio of 5 g/L, initial copper concentration of 5 mg/L, natural pH and a contact time of 2 h). Batch desorption experiments were carried out contacting copper-loaded sawdust with a HNO$_3$ 0.1 M solution at a solid/liquid ratio of 50 g/L. The samples were shaken at 25 °C and 400 rpm in an orbital shaking bath (VWR Incubating Mini Shaker) for 30 min. Then, the sawdust was separated by vacuum filtration with 1.2 μm glass microfiber filters and the liquid sample was analyzed by atomic absorption spectrophotometry as previously explained. After desorption, the sawdust was washed with distilled water several times to remove any acid residue, measuring the pH of the water after washing until reaching pH of distilled water. Four adsorption/desorption cycles were performed.

Desorption and regeneration efficiencies were calculated using Eq. (14) and Eq. (15), respectively:

$$\text{Desorption } \textit{efficiency} \, (\%) = \left[1 - \left(\left(m_a - m_d \right) / m_a \right) \right] \times 100 \tag{14}$$

$$\text{Regeneration } \textit{efficiency} \, (\%) = m_a \text{ on a specific cycle} / m_a \text{ in the first cycle} \tag{15}$$

where m_a and m_d, respectively, are the mass of copper adsorbed at equilibrium and in the sample after desorption (mg), respectively, for every cycle.

3. Results and discussion

3.1. Characterization of the adsorbent material

The levels of trace metals in *Pinus radiata* sawdust (Table 2) are significantly lower than those of other tree parts of pine species from nearby locations, such as *Pinus pinaster* from Portugal (Viana et al., 2018). However, although the concentration ranges differ widely, the trends are the same. That is, the most abundant elements in both species are iron, manganese and aluminum, and in smaller proportions are arsenic, cadmium, chromium, or lead. Moreover, the large amounts of aluminum or iron found in PS suggest that the presence of certain elements in the sawdust can be due to the contact of the wood surface wood with processing machines (Akhouairi et al., 2019). Based on the results, the possible interference of the metals present in the sawdust in the adsorption process was dismissed due to the low levels found.

As mentioned above, SEM and EDX analysis of the pine sawdust were performed in a previous work (sent to publication). Thereby, as an example, Figs. 1a and 2a show, respectively, one SEM image before adsorption and the corresponding results of the EDX analysis. After copper adsorption, changes in the biomass were detected (Figs. 1b and 2b, respectively). Thus, SEM shows that the sawdust surface became rougher after adsorption. Moreover, the porosity seems to keep still low, which suggests that in this case porosity does not play an important role in adsorption compared to other more porous materials. Finally, EDX analysis confirmed copper adsorption as copper weight % increased from 0.3 (Fig. 2a) to 0.93 (Fig. 2b) after adsorption. Additionally, the decrease in calcium, potassium, and magnesium weight % suggests that ion exchange is possibly one of the mechanisms involved in adsorption (Fawzy et al., 2022; Meez et al., 2021). No changes were detected for other elements such as carbon and oxygen.

FTIR analysis was used to evaluate the changes of functional groups in *Pinus radiata* sawdust, before and after copper adsorption. It can be observed that the pine spectrum (Fig. 3) shows peaks characteristic for lignocellulosic materials due to the presence of cellulose, lignin and hemicelluloses (Kovacova et al., 2019). According to literature (Xie et al., 2017; Vázquez et al., 2009) the broad and strong band at 3413 cm^{-1} may be due to overlapping of –OH and –NH stretching. Furthermore, peaks at 1157 and 1031 cm^{-1} (C–O stretching of ether and alcoholic and C–N stretching vibration) show the presence of hydroxyl and amine groups, respectively, and peaks at 1637 and 1735 cm^{-1} can be assigned, respectively, to a C=O stretching in carboxylic acids and their esters. The peak at 1510 cm^{-1} is attributed to amine groups, whereas the band at 2923 cm^{-1} can be due to C–H stretching and N–H bending. Finally, the

Table 2

Heavy metal concentration (mg/kg) in *Pinus radiata* sawdust compared to *Pinus pinaster* wood and bark stem (Viana et al., 2018).

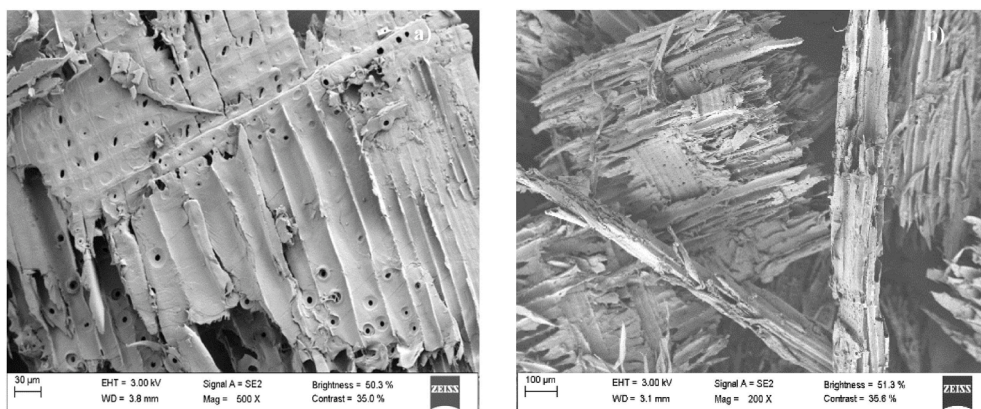| Pine species	Fe	Al	As	Cd	Pb	Co	Cu	Cr	Mn	Zn	Ni
Pinus radiata (this study)	552.6	43.6	0.02	0.03	0.2	0.1	1.0	0.2	111.6	11.5	0.2
Pinus pinaster (wood stem)	29,375.0	5884.4	3.8	0.9	13.4	17.1	926.3	109.4	9750.0	1250.0	37.5
Pinus pinaster (bark stem)	9794.0	8231.2	3.0	2.1	0.4	26.3	85.1	8.5	7239.0	1618.1	21.3

Fig. 1. SEM image of sawdust before (sent to publish) (a) and (b) after copper adsorption (Co: 45 mg/L, adsorbent dose: 12.5 g/L, pH: 7, contact time: 2 h).
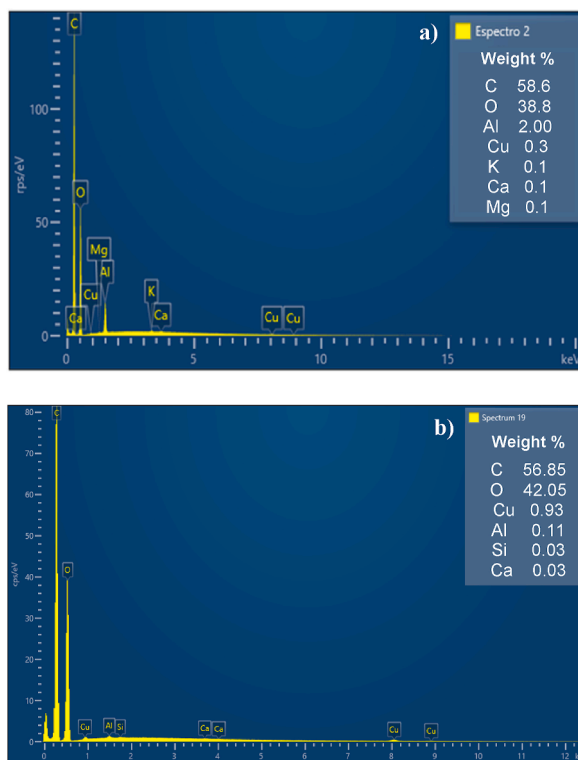

Fig. 2. EDX analysis of sawdust before (sent to publish) (a) and (b) after copper adsorption (Co: 45 mg/L, adsorbent dose: 12.5 g/L, pH: 7, contact time: 2 h).

peaks in the range of 1300–1400 cm^{-1} can be assigned to the link between the oxygen and the carbon in the cellulose (Andalia et al., 2020). It was demonstrated that many of these functional groups identified in the spectra as the carboxyl, hydroxyl and amine ones are involved in the copper adsorption (Xie et al., 2017; Vázquez et al., 2009). Although FTIR spectra before and after adsorption are similar (Fig. 3), it can be observed that, in general, peaks diminished in absorbance after copper binding, which can indicate that those groups participated via complexation and/or ion exchange as mentioned previously (Mongiovˆí et al., 2022).

With respect to XRD analysis, the diffractograms for pine sawdust before and after copper adsorption are shown in Fig. 4. Peaks corresponding to cellulose in its amorphous and crystalline forms, and to lignin and hemicelluloses, the amorphous material (Bala and Mondal, 2018), were observed. Thus, the peak of the crystalline plane was found at $2\theta \approx 22°$, and the lowest value of the amorphous region was at $2\theta \approx 16°$. The intensity of crystalline cellulose was practically unaffected by copper adsorption, being the crystallinity index (CI) for raw and copper loaded sawdust, 0.42 and 0.41, respectively. These low values indicate the important contribution of the amorphous part in the sawdust structure.
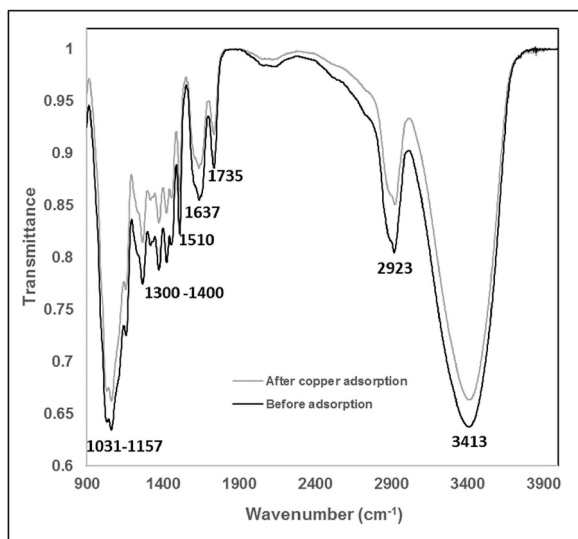
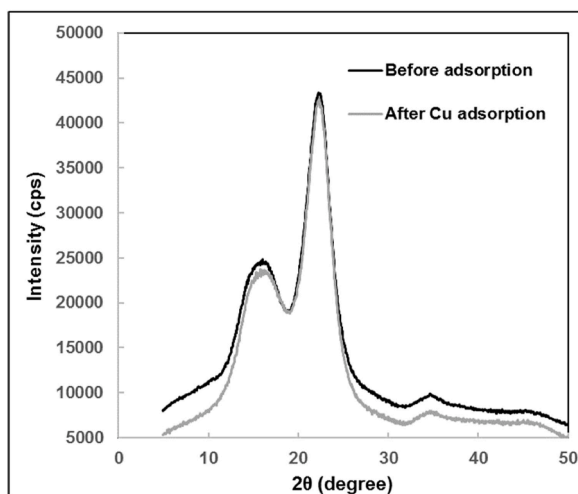**Fig. 3.** FTIR spectra of pine sawdust before and after copper adsorption.

Fig. 4. XRD diffractograms of pine sawdust before and after copper adsorption.

3.2. Influence of different parameters on copper adsorption

3.2.1. Effect of contact time

Firstly, the effect of contact time on copper adsorption was studied at the natural pH (5.4) for a 5 mg/L initial concentration and adsorbent dose of 1 g/L. The results shown in Fig. 5 demonstrated that copper adsorption was relatively fast, achieving a 36% adsorption efficiency in 15 min, and equilibrium conditions (42% adsorption efficiency) were attained in 1 h. Increasing the adsorbent dose to 50 g/L, the adsorption equilibrium was attained also in 1 h and the adsorption efficiency rose to 80%.

The experiments performed with a higher initial concentration of 45 mg/L at 1 and 50 g/L of adsorbent doses showed the same trend of fast adsorption in the first minutes, also reaching equilibrium in approximately 1 h. Nevertheless, for 1 g/L a low adsorption efficiency was obtained (13.5%), whereas when the adsorbent dose was increased to 50 g/L, the efficiency increased to 84.0%. However, at this dose the equilibrium adsorption efficiency decreased to 26% when the copper initial concentration was raised to 300 mg/L, although the equilibrium time was kept at 1 h.

In addition, for all experiments the equilibrium time seemed to be independent of the initial concentration of the metal. This behavior was also found in other studies (Geng et al., 2018; Taman et al., 2015).

High adsorption rates in the first minutes were also found for other biosorbents (Lim et al., 2008; Mannaï et al., 2021; Taty-Costodes et al., 2003). This behavior can be related to the adsorption mechanism that is affected by the initial metal concentration and the available adsorbent actives sites. When the adsorption starts, a large part of the adsorbent surface is available and there is a high concentration of the metal that is still not adsorbed which favors the mass transfer. As the adsorption process takes place, the adsorbent surface becomes more saturated, so there are fewer and harder accessible active sites. In addition, the low concentration gra-
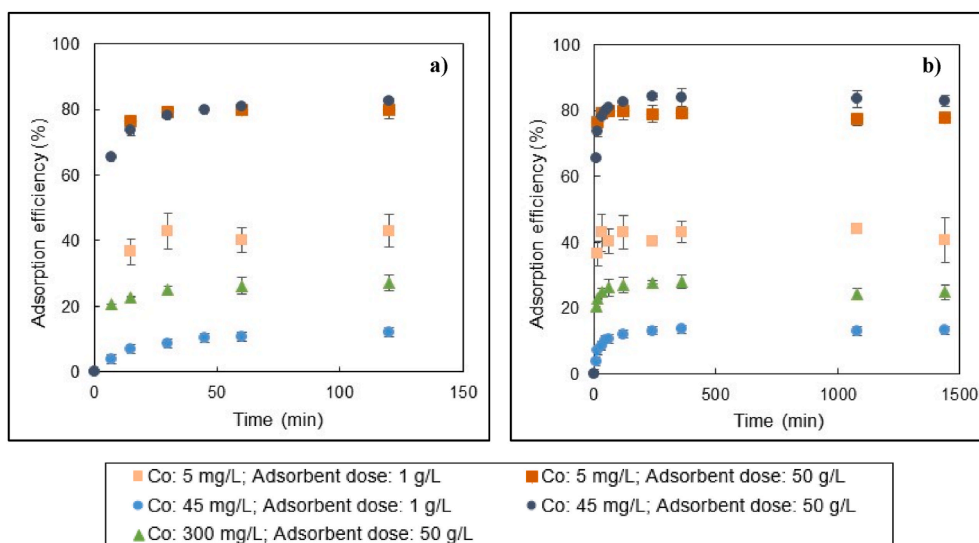
Fig. 5. Effect of contact time on Cu^{+2} adsorption efficiency at natural pH until 24 h (a) and (b) at the first 2 h (C_o: 5–300 mg Cu^{+2}/L, adsorbent dose: 1–50 g/L).

dient lowers the driving force. All this entails that the metal removal rate increases more slowly till equilibrium (Meez et al., 2021; Sahmoune and Yeddou, 2016).

3.2.2. Effect of the adsorbent dose

As expected, the removal efficiency increased with increasing the adsorbent dose from 1 to 10 g/L (Fig. 6) due to the higher availability of binding sites, but the change being much more pronounced from 1 to 5 g/L. However, from 10 to 50 g/L a decrease was observed that may be explained by overlapping adsorption sites or particle interactions such as aggregation, leading to a decrease in the adsorbent surface area (Sahmoune and Yeddou, 2016).

At 5 g/L an equilibrium adsorption efficiency of 82.6% (adsorption capacity 0.72 mg/g) was reached which was not significantly improved by increasing the adsorbent dose to 10 g/L. For this reason, 5 g/L was the dose selected to continue experimentation.

3.2.3. Effect of initial metal concentration

At the adsorbent dose previously selected (5 g/L) and natural pH the effect of the initial metal concentration was studied in a range that ensure compliance with regulation standards (Delgado Sancho et al., 2016) (1 and 5 mg/L). The best adsorption efficiency (91%) was achieved at 1 mg/L (Fig. 7) demonstrating that reducing initial concentration has a good effect on adsorption.
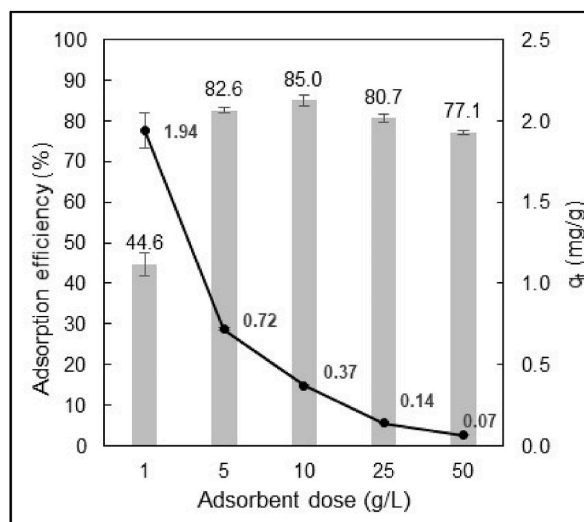

Fig. 6. Effect of pine sawdust dose on Cu^{+2} adsorption efficiency (Co: 5 mg Cu^{+2}/L, natural pH, contact time: 2 h).
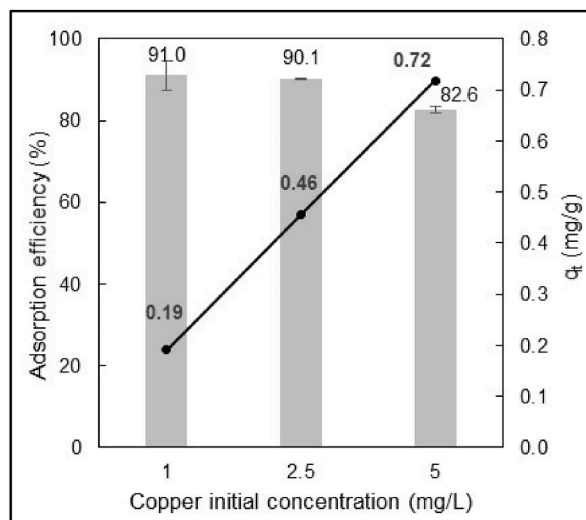
Fig. 7. Effect of copper initial concentration on Cu^{+2} adsorption efficiency (adsorbent dose: 5 g/L, natural pH, contact time: 2 h).

Therefore, the decrease in the adsorption efficiency observed with the rise of the copper concentration can be explained by the adsorbent saturation. However, the opposite effect was found in the adsorption capacity (Fig. 7) which can be explained by the presence of more metal ions available to interact with the adsorption sites (Meez et al., 2021).

3.2.4. Effect of pH

One of the most important factors controlling the adsorption is pH, especially for metals, because it is related to metal speciation. Moreover, pH also affects other aspects such as the adsorption capacity or the surface charge of the adsorbent (Wu et al., 2014).

Regarding metal speciation, there are a great diversity of speciation plots for metals as a function of pH. For that reason, a copper speciation plot as a function of pH was generated with MINTEQ 3.0 (Fig. 8). Although there may be differences due to temperature, concentration, etc., most authors agree that the predominant species is Cu^{+2} below pH = 4–5. When pH rises above 6, the amount of $Cu(OH)^{+}$ species starts to increase and $Cu(OH)^{+}$ and $Cu(OH)_2{}^{2+}$ are the dominant species at pH = 6–7. Close to pH = 8, precipitation of $Cu(OH)_2$ occurs and at pH greater than 10, new species such as $Cu(OH)^{3-}$ or $Cu(OH)_4{}^{2-}$ begin to appear (Sočo and Kalembkiewicz, 2015; Wu et al., 2014). Consequently, pH plays an important role in the choice of the mechanism of metal removal (adsorption or precipitation). However, in certain pH ranges it's difficult to establish the removal mechanism, even some authors concluded that micro-precipitation occurs during the biosorption process (Abdolali et al., 2014).

The increase of the removal percentage with increasing pH up 7 (Fig. 9) could be partially due to the presence of other species different from Cu2 + as mentioned earlier. The hydrated species of the metal ions such as Cu(OH) + and Cu(OH)2 (aq) have more mobility than Cu + 2 due to their smaller size because of their lower load. Thus, for hydrolyzed species, mass transfer resistance could be lower which allows a fast diffusion throughout the pores of the adsorbent and the probability of interaction is higher (Li et al., 2011; Xiao et al., 2004).
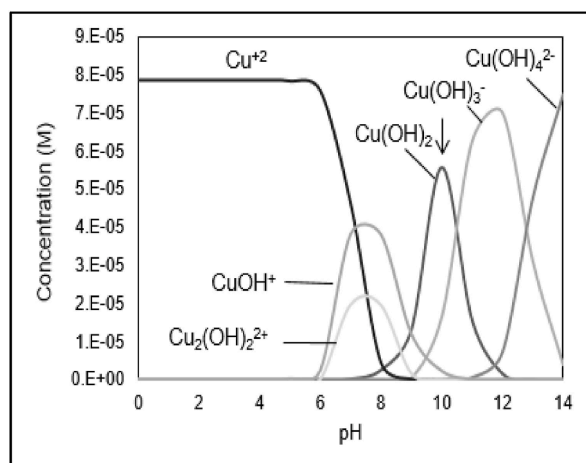

Fig. 8. Copper speciation diagrams of 5 mg Cu^{+2}/L in MINTEQ 3.0 software.
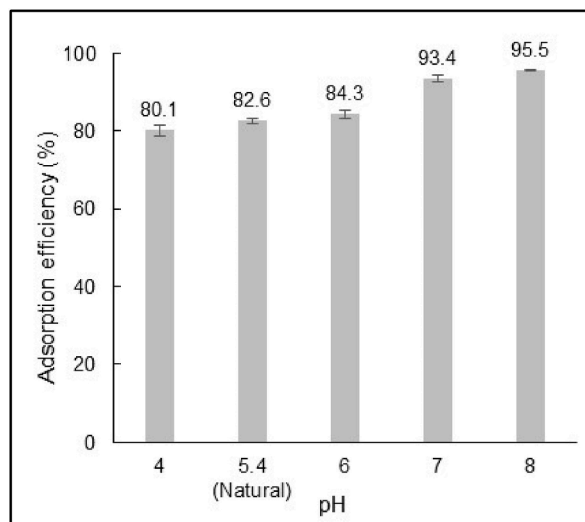
Fig. 9. Effect of pH on Cu^{+2} adsorption efficiency (Co: 5 mg Cu^{+2}/L, adsorbent dose: 5 g/L, contact time: 2 h).

The point of zero charge (pH_{PZC}) of the adsorbent is another factor that helps to explain the change in the adsorption efficiency with the solution pH. pH_{PZC} is the pH value for which the net charge on the adsorbent surface is zero. That is, at pH < pH_{PZC} = 4.8, the sawdust surface is positively charged and there is competition between H^+ and Cu^{+2} for the adsorption sites of the adsorbent, hence, repulsion exists. On the contrary, at pH higher than pH_{PZC}, the surface is negatively charged due to deprotonation, which favors the electrostatic attraction between Cu^{+2} and PS surface improving the adsorption percentage (Wu et al., 2014).

It was proved that adsorption efficiency increases with pH (Fig. 9), a behavior expected as most experiments were performed above pH_{PZC} and due to the increase of hydrated forms at the pH range essayed. Furthermore, below the point of zero charge, there were experiments without adsorption, like pH = 2. Regarding pH = 8, an adsorption efficiency of 95.5% was achieved but there were signs of precipitation. Consequently, based on the results obtained, pH = 7 was selected as the optimal pH reaching a 93.4% adsorption efficiency.

Moreover, after adsorption it was found that, in general, the final pH in filtrate was lower than the initial pH of the copper solution, which suggests again the existence of ion exchange (Sočo and Kalembkiewicz, 2015).

3.2.5. Adsorption optimization

The influence of the adsorbent dose (X_1) and initial concentration (X_2) on adsorption efficiency was analyzed using a Doehlert experimental design at two different pH, 7 (Y_1) and the natural pH (Y_2). Natural pH offers the advantage that it is possible to use the PS without treatment and microprecipitation is also avoided.

The analysis of variance (Table S1) showed that both regressions models were statistically significant at a 95% confidence level with R^2 values of 0.85 for pH = 7 and 0.96 for the natural pH which indicates a satisfactorily fit between the experimental values of the adsorption efficiency (Y_{exp}) and the predicted ones (Y_{cal}) (Table 3). At pH = 7 only the linear effect of the dose and the initial concentration of copper were significant (Eq. (16)) while at natural pH, the quadratic effect of concentration must also be considered (Eq. (17)).

$$Y_1 (\%) = 76.06 + 6.99X_1 - 11.89X_2 \tag{16}$$

Table 3
Doehlert matrix for the optimization of copper adsorption efficiency at pH 7 (Y_1) and natural pH (Y_2).

N	Adsorbent dose (g/L) (X_1)	Initial copper concentration (mg/L) (X_2)	Adsorption efficiency (%) (Y_1)		Adsorption efficiency (%) (Y_2)	
			$Y_{1, exp}$	$Y_{1, calc}$	$Y_{2, exp}$	$Y_{2,calc}$
1	15 (1)	25 (0)	88.55 ± 1.37	83.05	46.13 ± 0.06	45.56
2	12.5 (0.5)	45 (0.866)	68.09 ± 0.20	69.25	23.24 ± 1.16	29.88
3	5 (−1)	25 (0)	71.89 ± 0.36	69.07	19.66 ± 1,72	26.07
4	7.5 (−0.5)	5 (−0.866)	84.38 ± 3.03	82.87	72.29 ± 2.93	71.95
5	12.5 (0.5)	5 (−0.866)	85.71 ± 0.13	89.86	81.36 ± 0.44	81.70
6	7.5 (−0.5)	45 (0.866)	60.79 ± 0.16	62.26	26.78 ± 0.33	20.14
7	10 (0)	25 (0)	71.44 ± 0.44	76.06	37.71 ± 0.77	35.82
8	10 (0)	25 (0)	74.06 ± 1.59	76.06	35.84 ± 0.88	35.82
9	10 (0)	25 (0)	79.64 ± 0.57	76.06	39.74 ± 3.05	35.82

$$Y_2\,(\%) = 35.82 + 9.74X_1 - 29.92X_2 + 20.14X_2^2 \tag{17}$$

The response surfaces for adsorption efficiency as a function of adsorbent dose and initial concentration at pH 7 and natural pH are shown in Fig. 10 a and b, respectively. As can be appreciated, in both cases, the dose has a positive effect, so its increase improves the removal of copper, while the initial concentration has a negative effect, so its increase results in a lower adsorption efficiency. These results support the conclusions of the study of the main factors that affect copper adsorption.

Comparing the effect of both variables, the most significant is the copper initial concentration, especially working at the natural pH (Table S1). This can be explained by the quadratic effect which makes higher the reduction of the adsorption efficiency at elevated concentrations. Moreover, the effect of the dose at natural pH is slightly less significant (Table S1). The highest copper adsorption efficiency both at pH = 7 (93.4%) and at the natural pH (86.8%) was predicted at the highest adsorbent dose (15 g/L) and the lowest copper concentration (5 mg/L) for pH 7. Natural pH was selected for the following studies, as provide a relatively high adsorption rate that permit to reach limit values of legislation, reducing the use of chemicals.

3.3. Adsorption kinetics

Kinetic data for copper removal by PS at the natural pH were fitted to the pseudo-first order and pseudo-second order models and the kinetic parameters and correlation coefficients are shown in Table 4. The pseudo-second-order model fitted the data better ($R^2 > 0.99$) and, moreover, the adsorption capacities predicted (q_e calc) by this model were close to the experimental ones (q_e exp). Consequently, the adsorption of Cu^{+2} on pine sawdust can be described by a chemical sorption mechanism.

The intraparticle diffusion model was also applied and as seen in Fig. 11, under the conditions essayed the plots present various linear sections indicating that there is not only a rate-controlling step. In the initial part film diffusion is the controlling step and the metal ions are adsorbed on the most accessible sites, that is, the adsorbent exterior surface. Later, once these sites are saturated, the adsorbate entered into the pores and reacted with the actives sites, thus, demonstrating the occurrence of intraparticle diffusion as the rate-limiting process, that led to a decrease in the adsorption rate (Huang et al., 2018; Lima et al., 2015; Taty-Costodes et al., 2003; Turco and Malitesta, 2020).
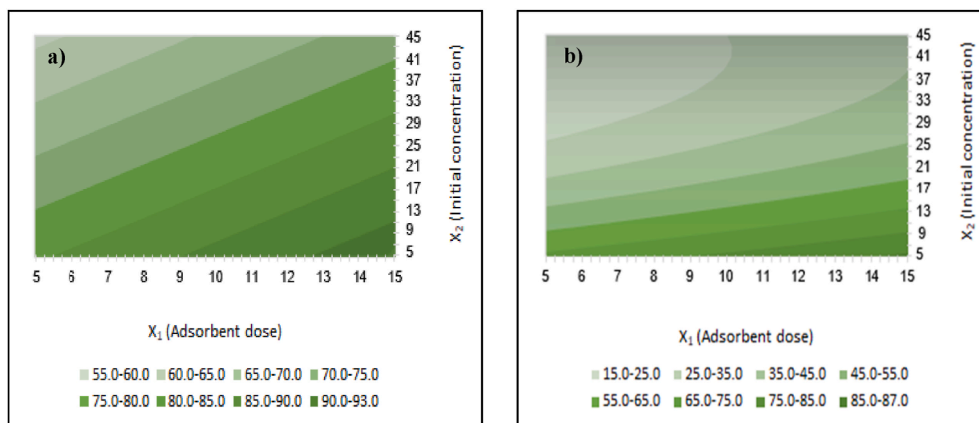

Fig. 10. Surface response graph for adsorption efficiency as a function of adsorbent dose and concentration at natural pH (a) and pH 7 (b) (contact time: 2 h).

Table 4
Pseudo-first-order and pseudo-second-order model parameters and correlation coefficients for adsorption of copper on pine sawdust at natural pH.

Initial concentration C_0 (mg/L)	Adsorbent dose (g/L)	q_e exp (mg/g) [a]	Pseudo first-order			Pseudo second-order		
			k_1 (min^{-1})	q_e calc (mg/g) [b]	R^2	k_2 (g mg^{-1} min^{-1})	q_e calc (mg/g) [b]	R^2
5	1	1.63	$9 \cdot 10^{-4}$	$9.7 \cdot 10^{-2}$	0.19	0.15	1.63	0.99
	50	$7.4 \cdot 10^{-2}$	$5 \cdot 10^{-4}$	$9 \cdot 10^{-4}$	0.16	5.38	$7.2 \cdot 10^{-2}$	0.99
45	1	9.79	$2.4 \cdot 10^{-3}$	6.52	0.98	$2.2 \cdot 10^{-3}$	9.87	0.99
	50	0.77	$1.6 \cdot 10^{-3}$	$6.6 \cdot 10^{-2}$	0.69	1.92	0.76	0.99
300	1	3.69	$1.4 \cdot 10^{-2}$	3.31	0.27	$4.7 \cdot 10^{-3}$	3.66	0.99
	50	1.68	$5 \cdot 10^{-4}$	0.27	0.07	$5.5 \cdot 10^{-2}$	1.52	0.99

[a] Experimental adsorption capacity.
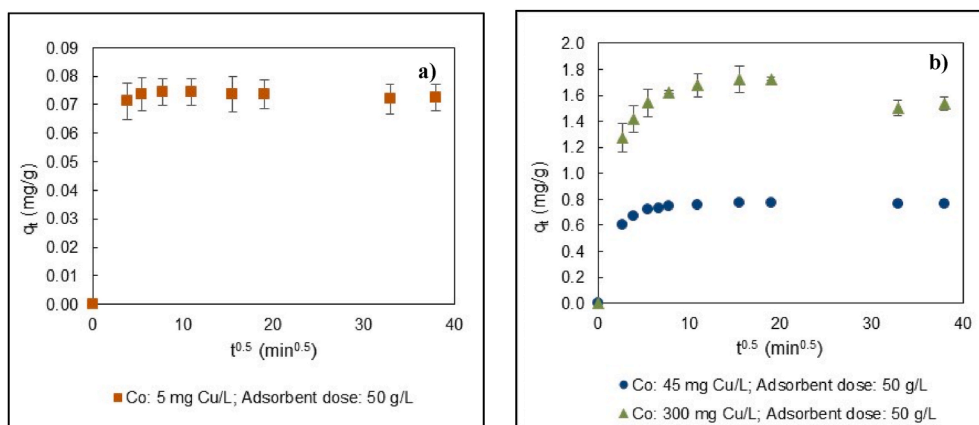[b] Predicted adsorption capacity.

Fig. 11. Application of intraparticle diffusion model at natural pH with initial copper concentrations of (a) 5 mg/L and an adsorbent dose of 50 g/L and (b) 5–300 mg/L with an adsorbent dose of 1–50 g/L.

3.4. Adsorption isotherms

Equilibrium data for copper removal by PS at 25 °C and natural pH were fitted to the Langmuir and Freundlich isotherm models and the parameters and correlation coefficients are shown in Table 5. Both models showed high correlation coefficients and could represent copper adsorption. A similar behavior has been reported for the adsorption of copper and zinc on pine bark (Amalinei et al., 2012) and for the adsorption of copper on wood sawdust (Sciban and Klasnja, 2004). Langmuir model with the highest correlation coefficient ($R^2 = 0.99$) suggests monolayer adsorption, with a maximum adsorption capacity (q_m) of 2.23 mg/g, which was compared with those of other unmodified biosorbents showing values of the same order (Table 6). Additionally, copper adsorption by pine sawdust has the advantage of being a faster and less energetically expensive process and no chemicals are needed to regulate pH.

Moreover, the dimensionless separation factor, R_L, is between 0 and 1, which indicates that adsorption is favorable. However, it should be noted that, as the concentration increases, R_L becomes closer to zero and, therefore, the process corresponds to irreversible equilibrium, which means that adsorption is stronger and consequently, the desorption is more difficult to perform (Hall et al., 1966; Weber and Chakravorti, 1974).

Table 5
Langmuir and Freundlich isotherms parameters for copper adsorption by *Pinus radiata* sawdust at natural pH.

	Langmuir Isotherm				Freundlich Isotherm		
	q_m (mg/g)	K_L (L/mg)	R_L	R^2	K_F (mg/g (mg/L)$^{-1/n}$)	N	R^2
Cu^{+2}	2.23	0.12	0.59 (5 mg/L) 0.02 (300 mg/L)	0.99	0.98	7.26	0.98

Table 6
Comparison of copper adsorption capacities for different low-cost unmodified adsorbents.

Adsorbent	Contact time (h)	T (°C)	Agitation (rpm)	pH	Concentration (mg/L)	Adsorbent dose (g/L)	q_m (mg/g)	Reference
Orange peel	24	30	180	5.5	0–24	1	4.75	Annadurai et al., 2003
Banana peel							3.65	
Rice husk	3	60	150	6	0–500	20	2.95	Aydin et al.,2008
Peanut hulls	168	30	150	5	0–200	10	2.95	Özsoy et al., 2007
Olive bone	1.66	25	No data	5	0–200	10	1.95	Blázquez et al., 2011
Pine bark							11.95	
Alamo sawdust	3	20	No data	4	0–190	5	2.54	Sciban et al., 2006
Fir sawdust							2.34	
sawdust	2	23	300	6.3	0–60	5	7.17	Larous et al., 2005
Poplar sawdust	3	25	200	4	0–50	2	6.58	Li et al., 2007
Birch wood sawdust	5.5	22	200	5	0–50	2	4.9	Grimm et al., 2008
Cherry sawdust	24	22	No agitation	4.1–4.4	0–150	10	2.16	Kovacova et al., 2020
Poplar sawdust							3.88	
Hornbeam sawdust							3.96	
Spruce sawdust							2.48	
Pinus radiata sawdust	2	25	100	Natural (5.4)	0–360	5	2.23	This study

Fig. 12 shows a comparison of experimental and calculated data fitted to Langmuir and Freundlich isotherms showing that the last one seems to explain better the adsorption process in the whole range studied. The Freundlich empirical parameters (Table 5) also confirmed copper and sawdust affinity (n > 1).

3.5. Desorption and adsorbent regeneration

Adsorbent regeneration is one of the most important factors to consider in an adsorption process, especially for industrial practice. It allows to develop a more economical and environmentally sustainable process by reducing costs, recovering the residual metals, and decreasing the production of hazardous wastes. The method selected for metal separation from sawdust was chemical desorption, which is the best option to maintain the main adsorbent properties and promote its reuse. This regeneration technique is also more effective, economical, and with less energy consumption than other processes, such as thermal regeneration or magnetic separation (Baskar et al., 2022).

Desorption can be carried out using different desorption agents, such as chelating agents (EDTA), bases (NaOH, NaNO$_3$), salts (NaCl, Na$_2$SO$_4$), acids (HNO$_3$, HCl, H$_2$SO$_4$), etc., however, for metals, acids are the most recommended ones (Afroze and Sen, 2018; Larous et al., 2005; Sahmoune and Yeddou, 2016). For that reason, in this study 0.1 M HNO$_3$ was used, which showed good results for the desorption of copper from various lignocellulosic biosorbents (Sciban and Klasnja, 2004; Witek-Krowiak, 2013).

The results for the copper desorption from copper loaded *Pinus radiata* sawdust, analyzing the influence of the desorption contact time for various initial metal concentrations of the adsorption stage, are shown in Fig. 13. As can be seen, the copper desorption effi-
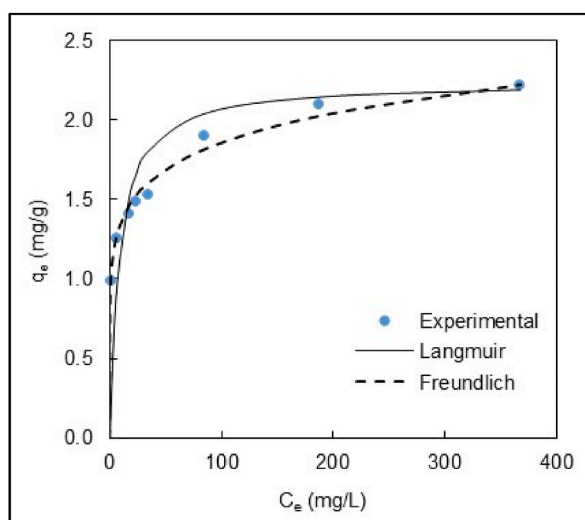

Fig. 12. Langmuir and Freundlich equilibrium adsorption isotherms (lines) and experimental data (points) (C$_o$: 5–360 mg Cu^{+2}/L, adsorbent dose: 5 g/L, natural pH, contact time: 2 h, T: 25 °C).
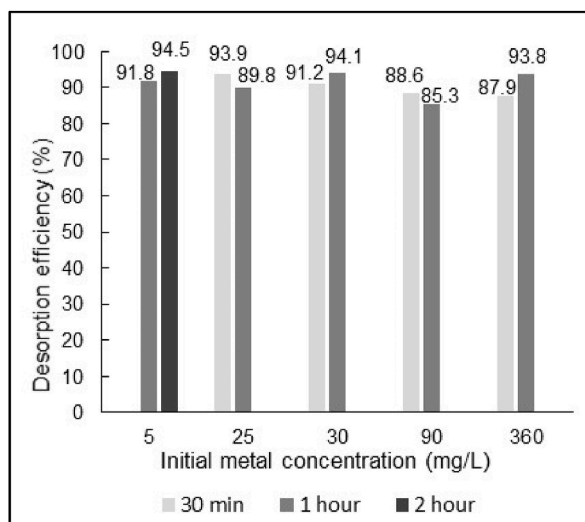

Fig. 13. Copper desorption with 0.1 M HNO$_3$ efficiencies at different initial cation concentrations and desorption times (solid-liquid ratio: 50 g/L; natural pH).

ciencies were high (average 91.1%), although the complete desorption was not achieved. This may be due to the difficulty of the copper ions to leave the adsorbent, getting trapped in their pores, or to the existence of strong bonds between the copper ions and the sawdust (Sciban and Klasnja, 2004).

Regarding the desorption time, 30 min are sufficient to achieve high desorption efficiencies (>88%), that is significantly shorter than the average of other studied that reported values greater than 2 h (Larous et al., 2005; Sciban and Klasnja, 2004; Sinyeue et al., 2022). Although increasing the contact time to 1 h generally offers greater efficiencies, these increases do not exceed 6%. Desorption efficiency was hardly influenced by the initial metal concentration of the adsorption stage, which contrasts with its effect on the adsorption process. These results could indicate that it is the equilibrium that controls the process.

Regeneration was tested by performing four adsorption–desorption cycles, whose regeneration efficiencies are shown in Fig. 14. The efficiency of sawdust recovery decreases to 29.3% after the fourth cycle. This decrease may be due to the fact that the sawdust is still loaded with copper, which difficults mass transfer by reducing the driving force or to irreversible alterations in the active sites due to the interaction between metal cations and functional groups of the adsorbent (Meez et al., 2021; Witek-Krowiak, 2013). No more cycles of adsorption-desorption were performed as four cycles were enough to test how many times the sawdust could be reused based on the loss of efficiency obtained in successive cycles. Thus, it is necessary to study if the regeneration of the adsorbent is profitable, as taking into account that the loss in efficiency was more than 50% in the second cycle, and sawdust is a cheap waste.

Anyway, the results obtained show that the subsequent management of the spent sawdust is possible without creating environmental or social problems. Once the metal is desorbed, several uses can be proposed for spent pine sawdust such as the amendment of low fertility soils, thermochemical processes for energy recovery, as raw material for capacitors and catalysts, where the presence of low residual metal contents doesn't suppose a problem, or the preparation of metal-based biochars (Abudi, 2018; Bădescu et al., 2018; Baskar et al., 2022; Fernández-González et al., 2019; Hossain et al., 2020; Huang et al., 2020; Ma et al., 2014). Regarding the desorbed metal, it could be recovered and reused, but the treatment process must be studied case by case, taking into account the great variety of copper species or copper chemical compounds used by the industrial processes and the compounds that may be present in the solution after desorption. Tassist et al. (2009) proposed the use of a combined desoption-electrolysis system which improved the desorption efficiency and permitted to recover the metal with high purity.

4. Conclusion

The present study concluded that *Pinus radiata* sawdust is a good adsorbent for the removal of Cu^{+2} from aqueous solutions under selected operational conditions. The optimal conditions to accomplish with current European discharge legislation (which normally has a maximum discharge limit of 5 mg/L), were copper initial concentrations below 15 mg/L, adsorbent dose between 5 and 15 g/L, contact time of 2 h and natural pH, to ensure that microprecipitation does not occur. The high efficiencies reached with low copper initial concentrations suggests that it would be advisable to pretreat the industrial effluents before adsorption to reduce the metal concentration, thus improving the process. Another option would be to use adsorption as an operation at the end of the wastewater treatment.

In addition, the desorption studies carried out with 0.1 M HNO_3 showed good efficiencies (average value of 91.1%), demonstrating that an environmentally acceptable operation can be achieved, as the copper can be recovered for later use in industry and the adsorbent can also be reutilized or subsequently managed without involving serious environmental impacts. Therefore, this process may be used to comply with the limitations imposed on the discharge of industrial wastewaters containing Cu^{+2}, while at the same time being a way of managing and valorizing pine sawdust. Adsorption of Cu^{+2} by *Pinus radiata* sawdust has proven to be faster and less
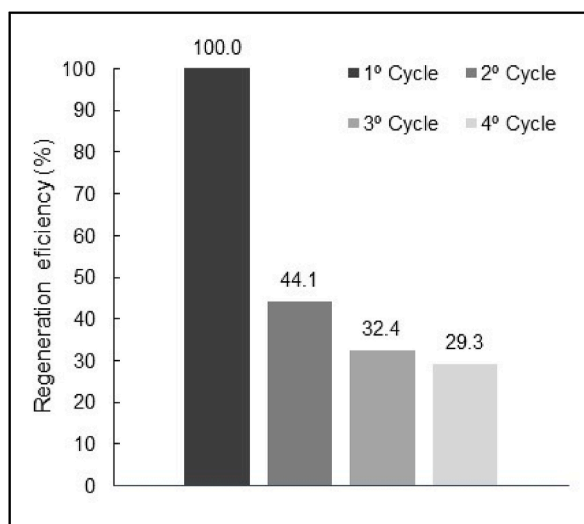

Fig. 14. Sawdust regeneration efficiency for 4 adsorption/desorption cycles (Adsorption: C$_o$: 5 mg/L; adsorbent dose: 5 g/L, natural pH, contact time: 2 h) (Desorption: 0.1 M nitric acid dose: 50 g/L; contact time: 30 min).

expensive than with other low-cost adsorbents. Moreover, this adsorbent should be easier to implement in a water purification process, since it does not require the wastewater pH correction, while reducing the use of reagents.

Future work will be focused on studying different modification treatments to increase sawdust adsorption performance. Additionally, much more work is necessary to scale up the process, studying not only continuous adsorption but also multicomponent systems, particularly with real wastewaters, and considering spent adsorbent disposal and metal recovery to add more economical value to the process.

Author statement

Clara Isabel Orozco: Conceptualization, Software, Formal Analysis, Investigation, Writing - Original Draft; **María Sonia Freire:** Conceptualization, Validation, Resources; Writing - Review & Editing, Supervision; **Diego Gómez-Díaz:** Conceptualization, Resources, Writing - Review & Editing, Supervision; **Julia González-Álvarez**: Conceptualization, Validation, Resources, Writing - Review & Editing, Supervision, Project administration.

Funding

Declaration of competing interest

The authors declare that they have no known competing financial interests or personal relationships that could have appeared to influence the work reported in this paper.

Data availability

Data will be made available on request.

Acknowledgements

Appendix A. Supplementary data

Supplementary data to this article can be found online at https://doi.org/10.1016/j.scp.2023.101016.

References

Abdolali, A., Guo, W.S., Ngo, H.H., Chen, S.S., Nguyen, N.C., Tung, K.L., 2014. Typical lignocellulosic wastes and by-products for biosorption process in water and wastewater treatment: a critical review. Bioresour. Technol. 160, 57–66. https://doi.org/10.1016/J.BIORTECH.2013.12.037.

Abudi, Z.N., 2018. Using sawdust to treat synthetic municipal wastewater and its consequent transformation into biogas. J. Ecol. Eng. 19 (5), 10–18. https://doi.org/10.12911/22998993/91271.

Acemioğlu, B., Alma, M.H., 2004. Sorption of copper (II) ions by pine sawdust. Holz als Roh- Werkst. 62 (4), 268–272. https://doi.org/10.1007/s00107-004-0480-3.

Afroze, S., Sen, T.K., 2018. A review on heavy metal ions and dye adsorption from water by agricultural solid waste adsorbents. Water Air Soil Pollut. 229 (7), 1–50. https://doi.org/10.1007/S11270-018-3869-Z.

Akhouairi, S., Ouachtak, H., Addi, A.A., Jada, A., Douch, J., 2019. Natural sawdust as adsorbent for the eriochrome black T dye removal from aqueous solution. Water Air Soil Pollut. 230 (8). https://doi.org/10.1007/s11270-019-4234-6.

Amalinei, R.L.M., et al., 2012. Investigations on the feasibility of Romanian pine bark wastes conversion into a value-added sorbent for Cu(II) and Zn(II) ions. Bioresources 7 (1), 148–160. https://doi.org/10.15376/biores.7.1.0148-0160.

Andalia, R., Julinawati, R., Helwati, H., 2020. Isolation and characterization of cellulose from rice husk waste and sawdust with chemical method. Jurnal Natural 20 (1), 6–9. https://doi.org/10.24815/jn.v20i1.12016.

Annadurai, G., Juang, R.S., Lee, D.J., 2003. Adsorption of heavy metals from water using banana and orange peels. Water Sci. Technol. 47 (1), 185–190. https://doi.org/10.2166/WST.2003.0049.

Aydin, H., Bulut, Y., Yerlikaya, Ç., 2008. Removal of copper (II) from aqueous solution by adsorption onto low-cost adsorbents. J. Environ. Manag. 87 (1), 37–45. https://doi.org/10.1016/J.JENVMAN.2007.01.005.

Bădescu, I.S., Bulgariu, D., Ahmad, I., Bulgariu, L., 2018. Valorisation possibilities of exhausted biosorbents loaded with metal ions –A review. J. Environ. Manag. 224, 288–297. https://doi.org/10.1016/j.jenvman.2018.07.066.

Bala, R., Mondal, M.K., 2018. Exhaustive characterization on chemical and thermal treatment of sawdust for improved biogas production. Biomass Convers. Biorefinery 8, 991–1003. https://doi.org/10.1007/s13399-018-0342-6.

Bansal, M., Garg, U., Singh, D., Garg, V.K., 2009. Removal of Cr(VI) from aqueous solutions using pre-consumer processing agricultural waste: a case study of rice husk. J. Hazard Mater. 162 (1), 312–320. https://doi.org/10.1016/J.JHAZMAT.2008.05.037.

Baskar, A.V., Bolan, N., Hoang, S.A., Sooriyakumar, P., Kumar, M., Singh, L., Jasemizad, T., Padhye, L.P., Singh, G., Vinu, A., Sarkar, B., Kirkham, M.B., Rinklebe, J., Wang, S., Wang, H., Balasubramanian, R., Siddique, K.H.M., 2022. Recovery, regeneration and sustainable management of spent adsorbents from wastewater treatment streams: a review. Sci. Total Environ. 822, 153555. https://doi.org/10.1016/J.SCITOTENV.2022.153555.

Basso, M.C., Cerrella, E.G., Cukierman, A.L., 2010. Cadmium uptake by lignocellulosic materials: effect of lignin content. Separ. Sci. Technol. 39 (5), 1163–1175. https://doi.org/10.1081/SS-120028577.

Bezerra, M.A., Santelli, R.E., Oliveira, E.P., Villar, L.S., Escaleira, L.A., 2008. Response surface methodology (RSM) as a tool for optimization in analytical chemistry. Talanta 76 (5), 965–977. https://doi.org/10.1016/J.TALANTA.2008.05.019.

BiPRO, 2012. Assessment and Guidance for the Implementation of EU Waste Legislation in Member States. European Commission Report, Brussels.

Blázquez, G., Martín-Lara, M.A., Dionisio-Ruiz, E., Tenorio, G., Calero, M., 2011. Evaluation and comparison of the biosorption process of copper ions onto olive stone and pine bark. J. Ind. Eng. Chem. 17 (5–6), 824–833. https://doi.org/10.1016/j.jiec.2011.08.003.

Briffa, J., Sinagra, E., Blundell, R., 2020. Heavy metal pollution in the environment and their toxicological effects on humans. Heliyon 6 (9), e04691. https://doi.org/10.1016/j.heliyon.2020.e04691.

Carreño-De León, M.C., Solache-Ríos, M.J., Cosme-Torres, I., Hernández-Berriel, M.C., Flores-Alamo, N., 2017. Adsorption of Cr(VI) by zea mays rachis. Rev. Mex. Ing. Quim. 16 (1), 261–269. https://doi.org/10.24275/rmiq/ia865.

Castro, A., Molina, F., Rojo, A., Sánchez, F., 1999. Manual de selvicultura del pino radiata en Galicia. Asociación Forestal de Galicia, Spain. http://www.agrobyte.com/publicaciones/pinoradiata/indice.html.

Delgado Sancho, L., Roudier, S., Brinkmann, T., Joint Research Centre, Institute for Prospective Technological Studies, 2016. Best Available Techniques (BAT) Reference Document for Common Waste Water and Waste Gas Treatment/management Systems in the Chemical Sector : Industrial Emissions Directive 2010/75/EU (Integrated Pollution Prevention and Control). Publications Office, Luxembourg. https://data.europa.eu/doi/10.2791/37535.

European Environment Agency, 2016. Environmental pressures of heavy metal releases from Europe's industry. European Enviroment Agency. In: EEA Briefing No 03/2018. Releases to the Environment from Europe's Industrial Sector. Publications Office of the European Union, Luxembourg, ISBN 978-92-9213-961-2. https://doi.org/10.2800/858619.

European Environment Agency, 2019. Industrial waste water treatment - pressures on Europes's environment. In: EEA Report No 23/2018. Publications Office of the European Union, Luxembourg, ISBN 978-92-9480-054-1. https://doi.org/10.2800/496223.

Fawzy, M.A., Darwish, H., Alharthi, S., Al-Zaban, M.I., Noureldeen, A., Hassan, S.H.A., 2022. Process optimization and modeling of Cd2 + biosorption onto the free and immobilized Turbinaria ornata using Box–Behnken experimental design. Sci. Rep. 12 (1), 1–18. https://doi.org/10.1038/s41598-022-07288-z.

Fernández-González, R., Martín-Lara, M.A., Moreno, J.A., Blázquez, G., Calero, M., 2019. Effective removal of zinc from industrial plating wastewater using hydrolyzed olive cake: scale-up and preparation of zinc-Based biochar. J. Clean. Prod. 227, 634–644. https://doi.org/10.1016/j.jclepro.2019.04.195.

Geng, Y., Zhang, J., Zhou, J., Lei, J., 2018. Study on adsorption of methylene blue by a novel composite material of TiO2 and alum sludge. RSC Adv. 8 (57), 32799–32807. https://doi.org/10.1039/c8ra05946b.

Gorgievski, M., Božić, D., Stanković, V., Štrbac, N., Šerbula, S., 2013. Kinetics, equilibrium and mechanism of Cu2 +, Ni2 + and Zn2 + ions biosorption using wheat straw. Ecol. Eng. 58, 113–122. https://doi.org/10.1016/j.ecoleng.2013.06.025.

Grimm, A., Zanzi, R., Björnbom, E., Cukierman, A.L., 2008. Comparison of different types of biomasses for copper biosorption. Bioresour. Technol. 99 (7), 2559–2565. https://doi.org/10.1016/j.biortech.2007.04.036.

Hall, K.R., Eagleton, L.C., Acrivos, A., Vermeulen, T., 1966. Pore- and solid-diffusion kinetics in fixed-bed adsorption under constant-pattern conditions. Ind. Eng. Chem. Fundam. 5 (2), 212–223. https://doi.org/10.1021/I160018A011.

Hossain, N., Bhuiyan, M.A., Pramanik, B.K., Nizamuddin, S., Griffin, G., 2020. Waste materials for wastewater treatment and waste adsorbents for biofuel and cement supplement applications: a critical review. J. Clean. Prod. 255, 120261. https://doi.org/10.1016/J.JCLEPRO.2020.120261.

Huang, Y., Lee, X., Grattieri, M., Macazo, F.C., Cai, R., Minteer, S.D., 2018. A sustainable adsorbent for phosphate removal: modifying multi-walled carbon nanotubes with chitosan. J. Mater. Sci. 53 (17), 12641–12649. https://doi.org/10.1007/S10853-018-2494-Y/FIGURES/7.

Huang, D., Li, B., Ou, J., Xue, W., Li, J., Li, Z., Li, T., Chen, S., Deng, R., Guo, X., 2020. Megamerger of biosorbents and catalytic technologies for the removal of heavy metals from wastewater: preparation, final disposal, mechanism and influencing factors. J. Environ. Manag. 261, 109879. https://doi.org/10.1016/J.JENVMAN.2019.109879.

Kajjumba, W.G., Emik, S., Öngen, A., Kurtulus Özcan, H., Aydın, S., 2018. Modelling of adsorption kinetic processes—errors, theory and application. In: Advanced Sorption Process Applications. IntechOpen Limited. https://doi.org/10.5772/INTECHOPEN.80495.

Kovacova, Z., Demcak, S., Balintova, M., 2019. Removal of copper, zinc and iron from water solutions by Spruce sawdust adsorption. Ekon. Srod. 3 (70), 64–74. https://doi.org/10.34659/2019/3/35.

Kovacova, Z., Demcak, S., Balintova, M., Pla, C., Zinicovscaia, I., 2020. Influence of wooden sawdust treatments on Cu(II) and Zn(II) removal from water. Materials 13 (16), 3575. https://doi.org/10.3390/MA13163575.

Larous, S., Meniai, A.H., Bencheikh Lehocine, M., 2005. Experimental study of the removal of copper from aqueous solutions by adsorption using sawdust. Desalination 185 (1–3), 483–490. https://doi.org/10.1016/j.desal.2005.03.090.

Li, Q., Zhai, J., Zhang, W., Wang, M., Zhou, J., 2007. Kinetic studies of adsorption of Pb(II), Cr(III) and Cu(II) from aqueous solution by sawdust and modified peanut husk. J. Hazard Mater. 141 (1), 163–167. https://doi.org/10.1016/j.jhazmat.2006.06.109.

Li, G., Zhao, Z., Liu, J., Jiang, G., 2011. Effective heavy metal removal from aqueous systems by thiol functionalized magnetic mesoporous silica. J. Hazard Mater. 192 (1), 277–283. https://doi.org/10.1016/J.JHAZMAT.2011.05.015.

Lim, J.-H., Kang, H.-M., Kim, L.-H., Ko, S.-O., 2008. Removal of heavy metals by sawdust adsorption: equilibrium and kinetic studies. Environ. Eng. Res. 13 (2), 79–84. https://doi.org/10.4491/eer.2008.13.2.079.

Lima, É.C., Adebayo, M.A., Machado, F.M., 2015. Kinetic and equilibrium models of adsorption. In: Carbon Nanostructures. Springer International Publishing, pp. 33–69. https://doi.org/10.1007/978-3-319-18875-1_3.

Lourizan, C.I.F., 2017. Pino insigne. https://lourizan.xunta.gal/es/centro/departamentos/departamento-de-silvicultura-y-mejora/recursos-geneticos/materiales-de-reproduccion/pino-insigne. (Accessed 31 March 2022).

Ma, W., Zong, P., Cheng, Z., Wang, B., Sun, Q., 2014. Adsorption and bio-sorption of nickel ions and reuse for 2-chlorophenol catalytic ozonation oxidation degradation from water. J. Hazard Mater. 266, 19–25. https://doi.org/10.1016/J.JHAZMAT.2013.12.007.

Mannaï, I., Sayen, S., Arfaoui, A., Touil, S., Guillon, E., 2021. Copper removal from aqueous solution using raw pine sawdust, olive pomace and their derived traditional biochars. Int. J. Environ. Sci. Technol. 19, 6981–6992. https://doi.org/10.1007/s13762-021-03629-z.

MARM (Ministerio de Medio Ambiente y Medio Rural y Marino), Canales Canales, C., Vara Blanco, A., Nava de Olano, B., Lucea Tortajada, J. In: Guía de Mejores Tecnicas Disponibles en España en el Sector de Tratamiento de Superficies Metálicas y Plásticas. Publications Office, Akasa S.L., Spain, ISBN 978-84-491-0917-1.

Meez, E., Rahdar, A., Kyzas, G.Z., 2021. Sawdust for the removal of heavy metals from water: a review. Molecules 26 (14), 4318. https://doi.org/10.3390/MOLECULES26144318.

Mongioví, Ch, Crini, G., Gabrion, X., Placet, V., Blondeau-Patissier, V., Krystianiak, A., Durand, S., Beaugrand, J., Dorlando, A., Rivard, C., Gautier, L., Lado-Ribeiro, A.R., Lacalamita, D., Martel, B., Staelens, J.-N., Ivanoska, A., Kostić, M., Heintz, O., Bradu, C., Raschetti, M., Morin-Crini, N., 2022. Revealing the adsorption mechanism of copper on hemp-based materials through EDX, nano-CT, XPS, FTIR, Raman, and XANES characterization techniques. Chemical Engineering Journal Advances 10, 100282. https://doi.org/10.1016/j.ceja.2022.100282.

Nordine, N., El Bahri, Z., Sehil, H., Fertout, R.I., Rais, Z., Bengharez, Z., 2014. Lead removal kinetics from synthetic effluents using Algerian pine, beech and fir sawdust's: optimization and adsorption mechanism. Appl. Water Sci. 6 (4), 349–358. https://doi.org/10.1007/S13201-014-0233-3.

Özsoy, H.D., Kumbur, H., Özer, Z., 2007. Adsorption of copper (II) ions to peanut hulls and Pinus brutia sawdust. Int. J. Environ. Pollut. 31 (1–2), 125–134. https://doi.org/10.1504/ijep.2007.015669.

Pérez-Marín, A.B., Zapata, V.M., Ortuño, J.F., Aguilar, M., Sáez, J., Lloréns, M., 2007. Removal of cadmium from aqueous solutions by adsorption onto orange waste. J. Hazard Mater. 139 (1), 122–131. https://doi.org/10.1016/J.JHAZMAT.2006.06.008.

Poland Ministry of Agriculture, 2013. Rulebook on limit values of waste water emissions. Official newsletter. . Nᵒ 80/2013./eli/sluzbeni/2013/80/1681.

Sahmoune, M.N., Yeddou, A.R., 2016. Potential of sawdust materials for the removal of dyes and heavy metals: examination of isotherms and kinetics. New Pub: Balaban 57 (50), 24019–24034. https://doi.org/10.1080/19443994.2015.1135824.

Sahoo, T.R., Prelot, B., 2020. Adsorption processes for the removal of contaminants from wastewater: the perspective role of nanomaterials and nanotechnology. Nanomaterials for the Detection and Removal of Wastewater Pollutants 161–222. https://doi.org/10.1016/B978-0-12-818489-9.00007-4.

Sciban, M., Klasnja, M., 2004. Study of the adsorption of copper(II) ions from water onto wood sawdust, pulp and lignin. Adsorpt. Sci. Technol. 22 (3), 195–206. https://doi.org/10.1260/0263617041503444.

Sciban, M., Klasnja, M., Škrbić, B., 2006. Modified softwood sawdust as adsorbent of heavy metal ions from water. J. Hazard Mater. 136 (2), 266–271. https://doi.org/10.1016/j.jhazmat.2005.12.009.

Semerjian, L., 2018. Removal of heavy metals (Cu, Pb) from aqueous solutions using pine (Pinus halepensis) sawdust: equilibrium, kinetic, and thermodynamic studies. Environ. Technol. Innovat. 12, 91–103. https://doi.org/10.1016/j.eti.2018.08.005.

Şentürk, İ., Alzein, M., 2020. Adsorption of acid violet 17 onto acid-activated pistachio shell: isotherm, kinetic and thermodynamic studies. Acta Chim. Slov. 67 (1), 55–69. https://doi.org/10.17344/ACSI.2019.5195.

Sinyeue, C., Garioud, T., Lemestre, M., Meyer, M., Brégier, F., Chaleix, V., Sol, V., Lebouvier, N., 2022. Biosorption of nickel ions Ni2 + by natural and modified Pinus caribaea Morelet sawdust. Heliyon 8 (2), e08842. https://doi.org/10.1016/J.HELIYON.2022.E08842.

Sočo, E., Kalembkiewicz, J., 2015. Removal of copper(II) and zinc(II) ions from aqueous solution by chemical treatment of coal fly ash. Croat. Chem. Acta 88 (3), 267–279. https://doi.org/10.5562/cca2646.

Taman, R., Ossman, M.E., Mansour, M.S., Farag, S.A., 2015. Metal oxide nano-particles as an adsorbent for removal of heavy metals. J. Adv. Chem. Eng. 5 (3). https://doi.org/10.4172/2090-4568.1000125.

Tassist, A., Lounici, H., Belhocine, C., Khelifa, A., Mameri, M., 2009. Removal and recovery of copper from aqueous solutions by Streptomyces rimosus biomass: enhancement of regeneration by desorption-electrolysis coupling. Desalination Water Treat. 3, 210–216. https://doi.org/10.5004/dwt.2009.462.

Taty-Costodes, V.C., Fauduet, H., Porte, C., Delacroix, A., 2003. Removal of Cd(II) and Pb(II) ions, from aqueous solutions, by adsorption onto sawdust of Pinus sylvestris. J. Hazard Mater. 105 (1–3), 121–142. https://doi.org/10.1016/j.jhazmat.2003.07.009.

Turco, A., Malitesta, C., 2020. Removal of phenolic compounds from olive mill wastewater by a polydimethylsiloxane/oxMWCNTs porous nanocomposite. Water 2020 12 (12), 3471. https://doi.org/10.3390/W12123471.

U.S. EPA (U.S. Environmental Protection Agency). Effluent guidelines implementation & compliance. In 40 CFR.Chapter I. Subchapter N. Parts 400-471. https://www.ecfr.gov/current/title-40/chapter-I/subchapter-N.

Vázquez, G., Calvo, M., Freire, M.S., González-Álvarez, J., Antorrena, G., 2009. Chestnut shell as heavy metal adsorbent: optimization study of lead, copper and zinc cations removal. J. Hazard Mater. 172, 1402–1414. https://doi.org/10.1016/j.jhazmat.2009.08.006.

Viana, H.F., dos, S., Rodrigues, A.M., Godina, R., Matias, J.C. de O., Nunes, L.J.R., 2018. Evaluation of the physical, chemical and thermal properties of Portuguese maritime pine biomass. Sustainability 10 (8), 1–15. https://doi.org/10.3390/su10082877.

Weber, T.W., Chakravorti, R.K., 1974. Pore and solid diffusion models for fixed-bed adsorbers. AIChE J. 20 (2), 228–238. https://doi.org/10.1002/AIC.690200204.

Witek-Krowiak, A., 2013. Application of beech sawdust for removal of heavy metals from water: biosorption and desorption studies. Eur. J. Wood Wood Prod. 71 (2), 227–236. https://doi.org/10.1007/s00107-013-0673-8.

World Health Organization, 2006. Recomendaciones (vol. 1). In: Guías para la calidad del agua potable World Health Organization. ISBN 92-4-354514-0. Ginebra.

Wu, Q., Chen, J., Clark, M., Yu, Y., 2014. Adsorption of copper to different biogenic oyster shell structures. Appl. Surf. Sci. 311, 264–272. https://doi.org/10.1016/J.APSUSC.2014.05.054.

Xiao, B., Thomas, K.M., 2004. Competitive adsorption of aqueous metal ions on an oxidized nanoporous activated carbon. Langmuir 20 (11), 4566–4578. https://doi.org/10.1021/la049712j.

Xie, R., Jin, Y., Chen, Y., Jiang, W., 2017. The importance of surface functional groups in the adsorption of copper onto walnut shell derived activated carbon. Water Sci. Technol. 76, 3022–3034. https://doi.org/10.2166/wst.2017.471.

Yao, W., Weng, Y., Catchmark, J.M., 2020. Improved cellulose X-ray diffraction analysis using Fourier series modeling. Cellulose 27, 5563–5579. https://doi.org/10.1007/s10570-020-03177-8.

ZDHC (Zero Discharge of Hazardous Chemicals Programme), 2015. Textile Industry Wastewater Discharge Quality Standards.